P4.12 AN ASSESSMENT OF SURFACE CLIMATE VARIABILITY IN A RECENT VERSION OF THE BUREAU OF METEOROLOGY RESEARCH CENTRE ATMOSPHERIC GCM

Harun A. Rashid* and Oscar Alves, Harry Hendon, and Lilia Deschamps
Bureau of Meteorology Research Centre, Melbourne, Victoria, Australia.

1. INTRODUCTION

Long-term means and interannual variability of a number of important climatic variables are examined in a simulation by a recent version of the Bureau of Meteorology Research Centre (BMRC) atmospheric GCM (hereafter BAM4). Many improvements have been introduced in this version of the GCM, including those based on recent advances in various physics parameterization schemes. BAM4 is expected to constitute the atmospheric component of the next version of the BMRC coupled model for climate applications and for seasonal prediction. In order to assess the likely impacts of these improvements on the coupled model simulations, we are analyzing the climatic variability of key surface variables simulated by BAM4 in a 19-year long AMIP2-style run. In this presentation, we compare the climatological means and interannual standard deviations of the monthly mean rainfall and 10-m zonal winds from BAM4 with those derived, respectively, from Xie-Arkin rainfall dataset (Xie and Arkin, 1997) and NCEP-DOE Reanalysis 2 (hereafter NCEP). In addition, we compare the EOF patterns representing the leading modes of variability of the observed and modelled rainfall and the 10-m zonal wind. Finally, correlations between the Niño 3.4 SST index and these variables are examined to determine how well the impacts of the El Niño–Southern Oscillation (ENSO) phenomenon is represented in the BAM4 simulation.

**Corresponding author address:* Dr. M. Harun Ar Rashid, Bureau of Meteorology Research Centre, Melbourne, Victoria, Australia. E-mail: h.rashid@bom.gov.au

2. MODEL DESCRIPTION

BAM4 has been run using observed time-dependent sea-surface temperature (SST) field and sea-ice data for 19 years corresponding to the period (1979-1997). The model is a global spectral model, with T47 horizontal resolution and 34 levels in the vertical. This version of the model incorporates the Fels-Schwarzkopf scheme (Schwarzkopf and Fels, 1991) for long-wave radiation, the mass flux convection scheme of Tiedtke (1989) for deep convection, the Rotstayn (1997) cloud scheme for stratiform clouds, and the Lott-Miller scheme (Lott and Miller, 1995) for orographic and gravity wave drag parameterization. The ECMWF land surface scheme and its boundary-layer scheme (Viterbo and Beljaars, 1995) are also used.

3. SEASONAL MEAN FIELDS

Long-term (1979-1997) averages of the seasonal mean 10-m zonal wind and rainfall were calculated for DJF and JJA seasons (Figures 1 and 2). The geographical distributions of the 10-m zonal winds, extracted from the BAM4 simulation and NCEP reanalyses, are very similar to each other. However, the model simulated zonal wind tends to be stronger than that in NCEP reanalyses almost everywhere over the globe, except in the polar and sub-polar regions where the opposite appears to be the case (Figs. 1c,f). The strongest differences occur over the northern subtropical Pacific and the Antarctic continent. The qualitative nature of these discrepancies between the BAM4 and NCEP zonal winds does not change with season.

The seasonal means of rainfall from the BAM4 simulation (Figs. 2a,b,c) and the Xie-Arkin

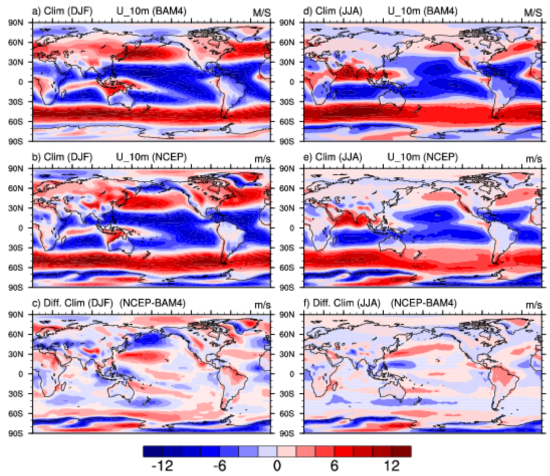

Figure 1: Long-term averages of seasonal mean 10-m zonal winds from the BAM4 simulation (a,d) and NCEP reanalyses (b,e). Differences between the NCEP and BAM4 averages are also presented (c,f). Results are shown for DJF (a,b,c) and JJA (d,e,f) seasons.

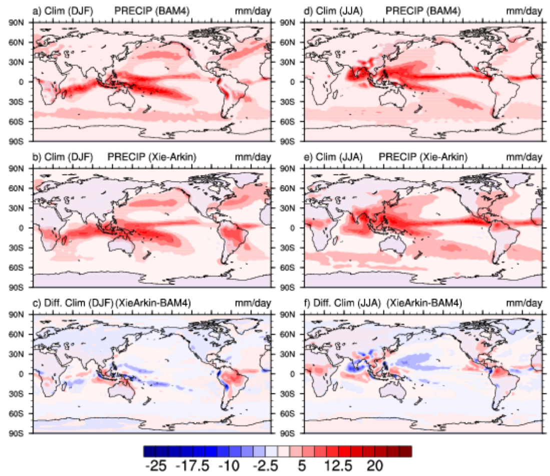

Figure 2: Long-term averages of seasonal mean rainfall from BAM4 (a,c) and Xie-Arkin dataset (b,d). Results are shown for DJF (a,b) and JJA (c,d) seasons.

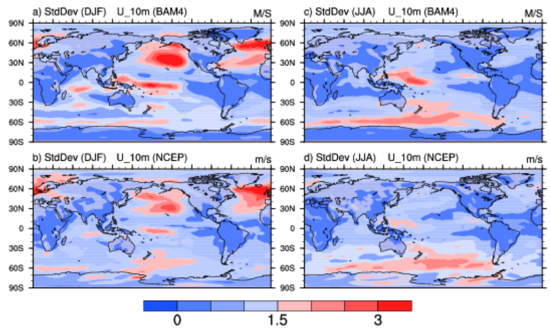

Figure 3: Interannual standard deviations of seasonal mean 10-m zonal wind from BAM4 (a,c) and NCEP reanalysis (b,d). Results are shown for DJF (a,b) and JJA (c,d) seasons.

dataset (Figs. 2 d,e,f) also show very similar spatial distributions. However, significant differences exist between the modelled and observed rainfalls, especially over the tropics (Figs. 2c,f). There, the BAM4 rainfall tends to be more intense than the observed over the western parts of the oceans; over the continents, however, BAM4 rainfall is clearly less than the Xie-Arkin rainfall. One notable exception, though, is the clear overestimation by the model of the monsoon rainfall over South India (and the surrounding oceanic area) during JJA. Overall, the seasonal mean rainfall and 10-m zonal wind simulated by BAM4 compare well with observations, although there is room for further improvements.

4. INTERANNUAL VARIABILITY

The interannual standard deviations of the seasonal mean 10-m zonal wind and rainfall are shown in Figs. 3 and 4, respectively. The spatial distribution of interannual zonal wind variability in the model (Figs. 3a, c) is very similar to that in the NCEP reanalysis (Figs. 3b, d). However, the modelled interannual variability is a bit too strong over the North Pacific and equatorial West Pacific compared with that in NCEP. This can be clearly seen during DJF. Over the Southern Ocean, the model tends to underestimate the zonal-wind variability around the date line. The model is only moderately successful in capturing the details of interannual rainfall variability. Although the large-scale spatial patterns are represented well (Fig. 4). the amplitude of rainfall variability in the model is a bit too large compared with observations. This is particularly visible over the western half of the equatorial Pacific during both seasons.

To gain further insight into the model simulated interannual variability, we computed three empirical orthogonal functions (EOFs) of the modelled and observed 10-m zonal wind and rainfall anomalies. Figures 5 and 6 show the leading EOF of the two variables for the DJF and JJA seasons. During DJF (Figs. 5a, b), the dominant interannual variability over the equatorial

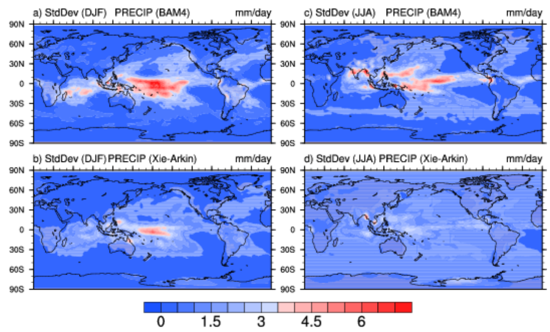

Figure 4: Interannual standard deviations of seasonal mean rainfall from BAM4 (a,c) and Xie-Arkin dataset (b,d). Results are shown for DJF (a,b) and JJA (c,d) seasons.

and North Pacific regions has analogous structures in BAM4 and NCEP, although the amplitude of variations over the North Pacific is larger in the model. Over the North Atlantic, however, the resemblance between BAM4 and NCEP is poor, primarily because the pattern of variability in the model is shifted towards higher latitudes with respect to that in NCEP. In addition, the structure of the BAM4 EOF in the Southern Hemisphere bears little resemblance with the structure of the NCEP EOF during DJF. During JJA, however, the similarity between the leading BAM4 and NCEP EOFs is good, especially in the Pacific and Indian Ocean sectors (Figs. 5c, d). Interestingly, the EOF structure in the Southern Hemisphere in JJA is reminiscent of the southern annular mode (Thomson and Wallace, 2000). The leading EOF

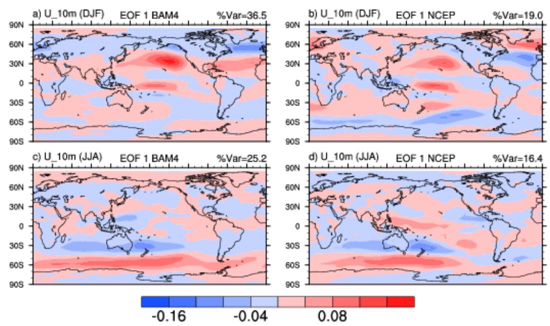

Figure 5: The leading EOF of the seasonal mean 10-m zonal wind anomalies from BAM4 (a,c) and NCEP reanalysis (b,d). Results are shown for DJF (a,b) and JJA (c,d) seasons.

of the simulated and observed rainfall anomalies is dominated by the variability over the tropical Pacific in both seasons (Fig. 6). A comparison between the BAM4 and NCEP EOF patterns shows that the model performs very well in simulating the interannual rainfall variability in this region.

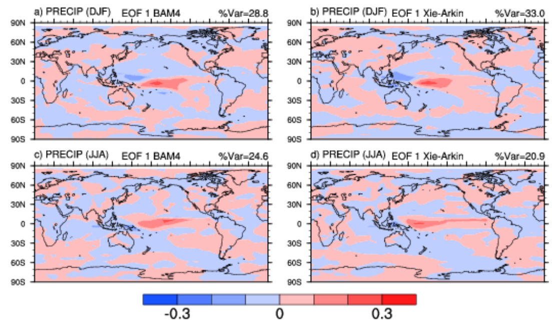

Figure 6: The leading EOF of the seasonal mean rainfall anomalies from BAM4 (a,c) and Xie-Arkin dataset (b,d). Results are shown for DJF (a,b) and JJA (c,d) seasons.

5. REPRESENTATION OF ENSO

We now examine the extent to which BAM4 simulates the ENSO cycle. This is done by preparing maps of correlation coefficients between the Niño 3.4 SST index and the interannual anomalies of the 10-m zonal wind and rainfall (Figs. 7 and 8). Over the tropical Pacific, where the ENSO effect is most direct, the zonal wind variability associ-

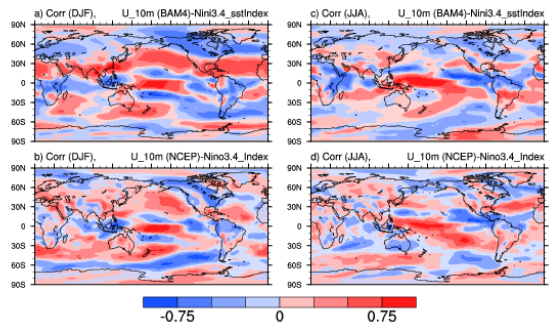

Figure 7: Correlations between Niño3.4 index and 10-m zonal wind from BAM4 (a,c) and NCEP reanalysis (b,d). Results are shown for DJF (a,b) and JJA (c,d) seasons.

ated with ENSO is represented well in the model. In other regions, however, the model has mixed success. In particular, among the regions where the model performance needs to be improved are tropical Africa and the adjacent north-west Indian Ocean, West Africa, south-west Australia and the South Indian Ocean. It may be noted that the representation of ENSO in BAM4 tends to be somewhat better during JJA than during DJF.

The results for the correlations between the Niño 3.4 SST index and the model simulated rainfall anomalies (Figs. 8a, c) are mixed, apart from

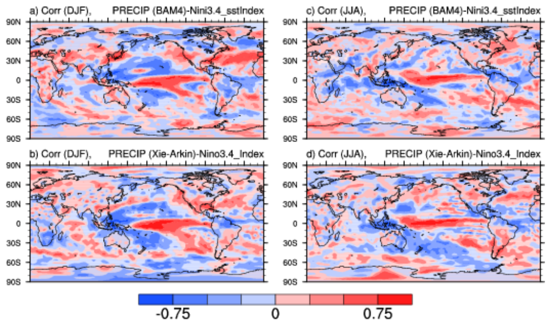

Figure 8: Correlations between Niño3.4 index and monthly mean rainfall from BAM4 (a,c) and Xie-Arkin dataset (b,d). Results are shown for DJF (a,b) and JJA (c,d) seasons.

in the tropical Pacific where both the magnitudes and the spatial pattern of the correlation show good agreement with observations (Figs. 8b, d). We should mention, however, that for a successful seasonal prediction of the ENSO-related rainfall variability over Australia, the models ability to simulate the ENSO-rainfall relationship needs to be improved further.

6. CONCLUDING REMARK

The results presented here were derived from a 19-year long simulation of BAM4. It would be desirable to have a longer simulation for an increased reliability of the results, as the time scales involved are in the interannual range. However, a brief comparison between these results and those computed from a 10-yr subset of the data indicates that the large-scale features are pretty robust. The results presented here suggest that the overall performance of BAM4 in simulating the long-term means and interannual variability of the 10-m zonal wind and rainfall is reasonably good. However, it is desirable that aspects of the model behavior continue to improve further in order to have an increased confidence in applying the model in various climate variability and change studies.

7. REFERENCES

Lott, F., and M. Miller, 1995: A new sub-grid scale orographic drag parameterization: its formulation and testing. ECMWF Technical Memorandum No. 218.

Rotstayn, L. D., 1997: A physically based scheme for the treatment of stratiform clouds and precipitation in large-scale models. 1: Description and evaluation of the microphysical processes. *Quart. J. Roy. Meteor. Soc.,* **123**, 1227–1282.

Schwarzkopf, M. D., and Fels, S. B., 1991: The simplified exchange method revisited an accurate, rapid method for computation of infrared cooling rates and fluxes. *J. Geophys. Res.,* **96**, 9075–9096.

Thompson, D. W. J., and J. M. Wallace, 2000: Annular modes in the extratropical circulation. Part I: Month-to-month variability. *J. Climate,* **13**, 1000–1016

.

Tiedtke, M., 1989. A comprehensive mass flux scheme for cumulus parameterization in largescale models. *Mon. Wea. Rev.,* **117**, 1779–1800.

Viterbo, P., and Beljaars, A.C.M. 1995. An improved land surface parameterization scheme in the ECMWF model and its validation. *J. Climate,* **8**, 2716–2748.

Xie, P. and P. A. Arkin, 1997: Global Precipitation: A 17-Year Monthly Analysis Based on Gauge Observations, Satellite Estimates and Numerical Model Outputs. *Bull. Amer. Meteor. Soc.,* **78**, 2539–2558.